# Absorption saturation measurement using the tapered optical nanofiber in a hot cesium vapor

**Zixuan Song (宋子旋)[1,2], Xingyu Yue (岳星宇)[3], Yu Luo (罗 宇)[3], Haodong Li (李好东)[3], and Yanting Zhao (赵延霆)[1,2,*]**

[1]*State Key Laboratory of Quantum Optics and Quantum Optics Devices, Institute of Laser Spectroscopy, Shanxi University, Taiyuan 030006, China*

[2]*Collaborative Innovation Center of Extreme Optics, Shanxi University, Taiyuan 030006, China*

[3]*College of Physics and Electronics Engineering, Shanxi University, Taiyuan 030006, China*

**Corresponding author: zhaoyt@sxu.edu.cn*

Received July 25, 2018; accepted December 20, 2018; posted online February 28, 2019

We report the observation of ultralow-power absorption saturation in a tapered optical fiber (TOF) mounted in a hot cesium (Cs) vapor in a vacuum chamber. The small optical mode area of TOF produces a great influence on optical properties, allowing optical interactions with nanowatt-level power. The comparison of transmission characteristics for the TOF system and free-space vapor is investigated at different input power and atomic density. The unique performance of the Cs-TOF system makes it a promising candidate in resonant nonlinear optical applications with ultralow power.

*OCIS codes: 190.4360, 300.6210, 350.4238.*
*doi: 10.3788/COL201917.031901.*

Most traditional nonlinear optical systems require high power laser fields, which contain large amounts of photons and are not easily modified for low-power operation[1–8]. Therefore, it is very important to study the new system with the ability of significant nonlinear effects with low power. The tapered optical fiber (TOF), as a narrow glass waveguide, has widespread availability on account of its high transmission and submicron beam waist[9–15]. The propagation of highly confined optical modes over interaction lengths is able to be achieved through a TOF[10,16]. A TOF can be conveniently connected to standard devices[17], which have higher compatibility for a compact all-fibered system and high capacity fiber networks. The tight confinement of the evanescent light field around the waist of the TOF[16,18,19] makes it an appropriate tool for studying nonlinear optics at an ultralow-power level[11,20,21]. These TOF systems have been used in a variety of fields, including nanowatt-level saturated absorption[12], electromagnetically induced transparency[20], investigation of interaction of the evanescent field with cold atoms[22], two-photon absorption[11], and low-power all-optical switching[23].

Remarkably, the low-power absorption spectrum has been observed using TOFs in different kinds of atomic vapor. The optical system with rubidium (Rb) vapor, including the observation of saturated absorption[12] and two-photon absorption within the nanowatt level[11], was reported. Nanowatt-level saturated absorption for TOFs mounted in gas of metastable Xe atoms has also been realized by Pittman *et al.*[21]. This study discussed the superiority of metastable Xe gas as an alternative to hot Rb atoms for ultralow-power nonlinear optics experiments using TOFs.

In this Letter, we experimentally investigate the ultralow-power absorption spectrum using a TOF mounted in a hot Cs-TOF system. We observe that the transmission measured through the TOF will saturate, even if input power is a few nanowatts. The experimental results are compared with those obtained by passing a free-space beam through a standard vacuum chamber, which needs about a milliwatt of power to achieve saturation. In addition, the atomic density also plays an important role in the absorption saturation. Through measurement and calculation, we found that atomic density increases with temperature, and our experiment demonstrates the relationship of the transmission of light with different atomic densities on the condition of unsaturated vapor pressure.

A schematic of the experimental setup is shown in Fig. 1. The left side of the diagram is the optical system, and the right side is the TOF system. The TOF is mounted in the vacuum chamber with cesium (Cs) vapor, which is the main component of the experiment. Our fiber is produced from a standard single-mode fiber using the "flame-brush" technique[24] with a hydrogen–oxygen flame. This technique allows for the implementation of any required TOF waist radius and its overall length. The whole fabrication of the nanofiber is calculated by simulating the pulling process on a computer and can be monitored in real time during drawing. In the experiment, the fiber has a final transmission of about 98% with a final diameter of about 503 nm and length of about 5 mm measured by a scanning electron microscope (SEM), as shown in the insert of Fig. 1. The TOF is connected to optical fibers outside the vacuum chamber through feedthroughs[25] using an oven to control the temperature of the vacuum chamber around 90°C. The vacuum system is pumped with a turbo pump. The background pressure after bake out is typically $5 \times 10^{-4}$ Pa. A valve could then be opened to introduce Cs vapor into the vacuum chamber.

 

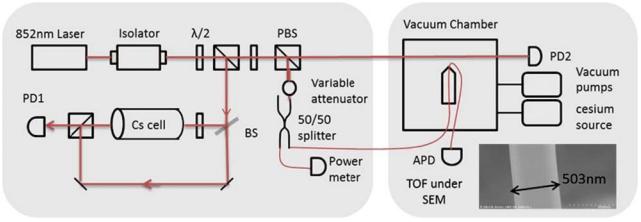


Fig. 1. A schematic of the experimental setup. The left side of the diagram is the optical system, and the right side is the TOF system. Photodiode detectors PD1 and PD2 are used to record the reference signal of the saturated absorption spectrum and the free-space beam respectively. The APD is used for the TOF signal. The image of the tapered nanofiber under the scanning electron microscope is also shown in the diagram. PD, photodiode; APD, avalanche photodiode; PBS, polarization beam splitter; BS, beam splitter; $\lambda/2$, half-wave plate.

The nanofiber is mounted in an aluminum heating base by the low-outgassing UV curable epoxy. Two thermocouples are placed on this heating base and chamber to monitor the temperature near the nanofiber and chamber. We notice that the transmission is affected almost immediately when Cs vapor is introduced into the vacuum chamber and decreases as the Cs vapor density is increased. There will be long-term accumulation of large amounts of Cs on the nanofiber, which would cause a significant loss of transmission through the fiber[26]. This often occurs when the temperature of the fiber is too low, or a high density of Cs atoms is produced. To reduce transmission loss, the temperature of the optical nanofiber heated by a ceramic heater is about 10°C higher than that of the vacuum chamber.

As shown in Fig. 1, the optical part of the system is driven by an 852 nm diode laser with the beam diameter of 2 mm. The combination of a half-wave plate ($\lambda/2$) and polarization beam splitter (PBS) can adjust the powers of the transmitted and reflected beams. Part of the beam passes through the Cs reference cell to obtain the saturated absorption spectrum (SAS) monitored by a photodiode (PD1). The other part of the beam that passes through the vacuum chamber is detected by PD2, named the free-space beam. The last part of the beam passes through the 50/50 splitter and is separated into two light signals: one beam is monitored by a power meter, and the other beam through the TOF is detected by a sensitive avalanche photodiode (APD). In the system, the variable attenuator before the fiber input coupler allows the input power to be reduced to the nanowatt level.

The performance of the TOF system was studied by continuously scanning the laser frequency across a range of 2 GHz. As shown in Fig. 2, the absorption spectrum for the transition from $6S_{1/2}$ to $6P_{3/2}$ has been observed by using a TOF. The experimental results show the normalized transmission variety as a function of the frequency detuning. Here, the transmission is defined to be the ratio of output power to input power. The spectral linewidths of the absorption spectrum in free-space and the TOF are affected by different factors, such as Doppler broadening and transit broadening.

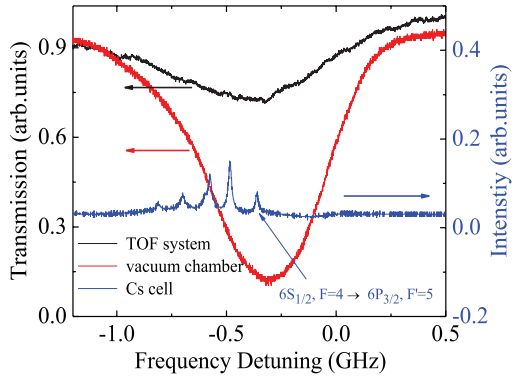


Fig. 2. Absorption signals of Cs D2 line for the TOF system (black) measured by the APD with the input power of 1 nW, and the vacuum chamber (red) measured by PD2 with the input power of 4.9 mW. The temperature of TOF is around 101°C. The Doppler-free saturated spectrum (blue) obtained by PD1 is used as a frequency reference.

The typical relationships between input power and transmission in a TOF system and in Cs vapor are shown in Fig. 3. The measured transmission is chosen to be the value at the transition from $6S_{1/2}$, $F = 4$ to $6P_{3/2}$, $F' = 5$ (shown in Fig. 2). Each set of the data is ensured to be measured at the same temperature. The transmission has the same trend in all cases. Within the low-power range, the transmission grows rapidly as the incident light

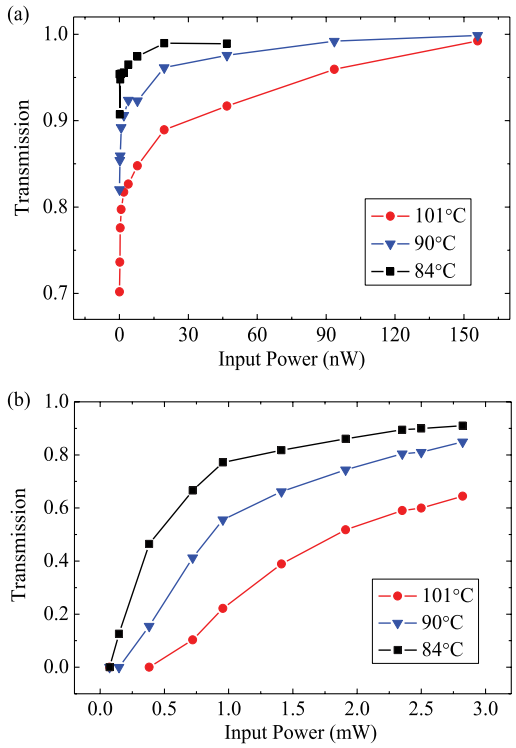


Fig. 3. Comparison of the measured transmission for (a) the TOF system and (b) free-space vapor under different temperatures.

increases. It will gradually stabilize as the power continuously increases. The saturation effect arises from the population of the excited state reaching the maximum[10–12]. To achieve the same transmission, free-space light requires milliwatts of power, whereas the TOF system only requires the level of nanowatt power. This means that it is easier to be saturated for the input power of the TOF, which is owed to the tighter evanescent field around the TOF and stronger coupling efficiency compared with the light in free-space. We notice that a quantitative analysis on the dependence of transmission on input power has been represented in Ref. [12] using Rb atoms. Comparing their measurement, we have the same order of power reaching saturated transmission for free-space vapor. However, the power reaching saturated transmission for the TOF is lower in our experiment, which arises from the large waist size of our nanofiber.

The atomic density is also a factor affecting the transmission. By increasing temperature, the density of the atoms in the vacuum chamber increases rapidly. This value can be estimated by the power difference between the input power and the output power of the free-space beam in Fig. 3(b). We derive the atomic density based on the Beer–Lambert law, $T = e^{-\sigma \cdot \rho \cdot l}$, where $T$ is transmission, $\rho$ is the number density, and $l$ is the path length of the light through the chamber; in our experiment, $l = 0.1$ m. $\sigma$ is the cross section of light and atom[27] and can be written as

$$\sigma = \frac{\sigma_0}{1 + I/I_{\text{sat}} + (2\Delta/\Gamma)^2}, \tag{1}$$

where $\Gamma$ is the decay rate of spontaneous radiation ($\Gamma = 3.28 \times 10^7$ s$^{-1}$). $I_{\text{sat}}$ is the saturation intensity of atoms ($I_{\text{sat}} = 2.7$ mW/cm$^2$), $\Delta$ is frequency detuning from resonant transition between $F = 4$ and $F' = 5$ and is chosen to be zero, and $\sigma_0$ is the resonant cross section ($F = 4 \rightarrow F' = 5$) ($\sigma_0 = 1.413 \times 10^{-9}$ cm$^2$)[28]. Our calculations show that the Cs atomic densities for the temperatures of 84°C, 90°C, and 101°C are $(3.1 \pm 0.6) \times 10^{14}$ m$^{-3}$, $(5.9 \pm 0.9) \times 10^{14}$ m$^{-3}$, and $(1.2 \pm 0.2) \times 10^{15}$ m$^{-3}$, respectively, which are much smaller than the saturated vapor pressure ($8 \times 10^{18}$ m$^{-3}$). It is noticed that these values are derived from the transmissions in the range of 0.3–0.7 for the deviation that is large when the transmission is too low (noise is large) or too high (saturation appears). We plot the relationship between atomic density and measured transmission in Fig. 4. The observable trend is that the transmission decreases as the atomic density increases. When the atomic density increases in the vaccum chamber, the photons in the evanescent field are more easily absorbed by the atoms per unit time that will induce the transmission to be lower.

In summary, we have observed the transmission spectra of Cs atoms using a TOF. We have found that with the increase of the input light power, transmission tends to stabilize, which is caused by saturation of the upper-level transition. By raising the temperature, the atomic density increases, inducing increases of the absorption capacity of photons and the reduction of transmission. In addition, we compare the performance of the "Cs-TOF" system and free-space vapor system. The power-dependent absorption saturation measurement for the TOF system has been achieved at very low pump power levels, which provides a useful tool for studying the nonlinear effect at ultralow power.

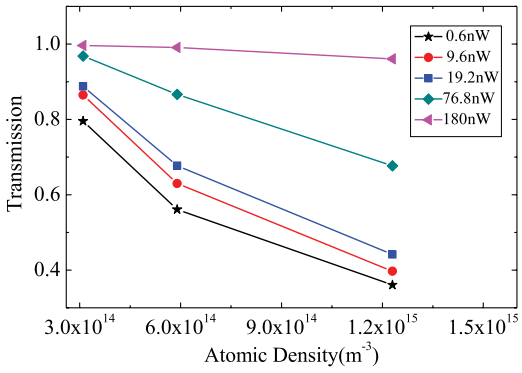


Fig. 4. Measured transmission for the TOF system as a function of atomic density under different input powers.

This work is supported by the National Key Research and Development program (No. 2017YFA0304203), National Natural Science Foundation of China (Nos. 61675120, 11434007, and 61875110), NSFC Project for Excellent Research Team (No. 61121064), Shanxi Scholarship Council of China, "1331 KSC", PCSIRT (No. IRT 13076), and Applied Basic Research Project of Shanxi Province (No. 201601D202008).

## References

1. D. Braun, J. Hoffman, and E. Tiesinga, Phys. Rev. A **83**, 62305 (2011).
2. R. Z. Vered, Y. Shaked, Y. Ben-Or, M. Rosenbluh, and A. Pe'er, Phys. Rev. Lett. **114**, 063902 (2015).
3. R. T. Willis, F. E. Becerra, L. A. Orozco, and S. L. Rolston, Phys. Rev. A **79**, 033814 (2009).
4. L. Duan, M. D. Lukin, J. I. Cirac, and P. Zoller, Nature (London) **414**, 413 (2001).
5. D. Petrosyan and M. Fleischhauer, Phys. Rev. Lett. **100**, 170501 (2008).
6. D. Petrosyan, G. Bensky, G. Kurizki, I. Mazets, J. Majer, and J. Schmiedmayer, Phys. Rev. A **79**, 040304(R) (2009).
7. S. Liang, Y. Xu, and Q. Lin, Chin. Opt. Lett. **15**, 090201 (2017).
8. K. Wang, W. Zhang, Z. Zhou, M. Dong, S. Shi, S. Liu, D. Ding, and B. Shi, Chin. Opt. Lett. **15**, 060201 (2017).
9. L. Stern, B. Desiatov, I. Goykhman, and U. Levy, Nat. Commun. **4**, 1548 (2013).
10. M. Lai, J. D. Franson, and T. B. Pittman, Appl. Opt. **52**, 2595 (2013).
11. S. M. Hendrickson, M. M. Lai, T. B. Pittman, and J. D. Franson, Phys. Rev. Lett. **105**, 173602 (2010).
12. D. E. Jones, J. D. Franson, and T. B. Pittman, J. Opt. Soc. Am. B **31**, 1997 (2014).
13. A. Goban, K. S. Choi, D. J. Alton, D. Ding, C. Lacroûte, M. Pototschnig, T. Thiele, N. P. Stern, and H. J. Kimble, Phys. Rev. Lett. **109**, 033603 (2012).

14. M. Kohnen, M. Succo, P. G. Petrov, R. A. Nyman, M. Trupke, and E. A. Hinds, Nat. Photon. **5**, 35 (2011).
15. T. A. Birks and Y. W. Li, J. Lightwave Technol. **10**, 432 (1992).
16. L. Tong, J. Lou, and E. Mazur, Opt. Express **12**, 1025 (2004).
17. J. Su, L. Cui, Y. Li, and X. Li, Chin. Opt. Lett. **16**, 041903 (2018).
18. F. L. Kien, J. Q. Liang, K. Hakuta, and V. I. Balykin, Opt. Commun. **242**, 445 (2004).
19. K. Okamoto, *Fundamentals of Optical Waveguides* (Academic, 2000).
20. S. M. Spillane, G. S. Pati, K. Salit, M. Hall, P. Kumar, R. G. Beausoleil, and M. S. Shahriar, Phys. Rev. Lett. **100**, 233602 (2008).
21. T. B. Pittman, D. E. Jones, and J. D. Franson, Phys. Rev. A **88**, 053804 (2013).
22. E. Vetsch, D. Reitz, G. Sagué, R. Schmidt, S. T. Dawkins, and A. Rauschenbeutel, Phys. Rev. Lett. **104**, 203603 (2010).
23. K. Salit, M. Salit, S. Krishnamurthy, Y. Wang, P. Kumar, and M. S. Shariar, Opt. Express **19**, 22874 (2011).
24. J. E. Hoffman, S. Ravets, J. A. Grover, P. Solano, P. R. Kordell, J. D. Wong-Campos, L. A. Orozco, and S. L. Rolston, AIP Adv. **4**, 067124 (2014).
25. E. R. L. Abraham and E. A. Cornell, Appl. Opt. **37**, 1762 (1998).
26. M. Fujiwara, K. Toubaru, and S. Takeuchi, Opt. Express **19**, 8596 (2011).
27. D. A. Steck, "Quantum and atom optics", 2017, http://steck.us/teaching.
28. D. A. Steck, "Cesium D line data", 2010, http://steck.us/alkalidata.